HHS Public Access

Author manuscript

Matrix Biol. Author manuscript; available in PMC 2018 October 01.

Published in final edited form as:

Matrix Biol. 2017 October ; 62: 28–39. doi:10.1016/j.matbio.2016.11.001.

Hyaluronan 35 kDa treatment protects mice from *Citrobacter rodentium* infection and induces epithelial tight junction protein ZO-1 *in vivo*

Yeojung Kim[1,*], **Sean P. Kessler**[1,*], **Dana R. Obery**[1], **Craig R. Homer**[1], **Christine McDonald**[1], and **Carol A. de la Motte**[1]

[1]Department of Pathobiology, Lerner Research Institute, Cleveland Clinic Foundation, Cleveland, OH

Abstract

Maintaining a healthy intestinal barrier, the primary physical barrier between intestinal microbiota and the underlying lamina propria, is critical for optimal health. Epithelial integrity is essential for prevention of the entrance of luminal contents, such as bacteria and their products, through the large intestinal barrier. In this study, we investigated the protective functions of biosynthetic, specific sized, hyaluronan around 35 kDa (HA35) on intestinal epithelium in healthy mice, as well as mice infected *Citrobacter rodentium*, an established model that mimics infection with a serious human pathogen, enteropathogenic *E. coli* (EPEC). Our results reveal that treatment with HA35 protects mice from *Citrobacter* infection and enhances the epithelial barrier function. In particular, we have found that HA35 induces the expression of tight junction protein zonula occludens (ZO)-1 in both healthy and *Citrobacter* infected mice, as demonstrated by immunoflurorescence and Western blot analyses. Furthermore, we determined that HA35 treatment enhances ZO-1 expression and reduces intestinal permeability at the early stages of dextran sulfate sodium (DSS)-induced colitis in mice. Together, our data demonstrate that the expression and functionality of tight junctions, is increased by HA35 treatment, suggesting a novel mechanism for the protection from *Citrobacter* infection.

Keywords

Hyaluronan; Tight junction protein; Colonic epithelium; Epithelial barrier; Infection

1. Introduction

The gastrointestinal tract is a major interface between the contaminated external environment and a sterile body, and functions in the digestion of food, the absorption of

Corresponding author: Carol A. de la Motte, [1]Department of Pathobiology, Lerner Research Institute, Cleveland Clinic Foundation, Cleveland, OH 44195, USA, Tel: (216) 444-5374, Fax: (216) 636-0104, delamoc@ccf.org.

[*]Y.K., and S.P.K contributed equally to this work.

water and nutrients, and the maintenance of an enormous population of largely beneficial bacteria, known as the microbiota. A healthy gastrointestinal tract is maintained by multiple host defense mechanisms that exist to protect the gut from constant microbial challenges. Dysregulation of the intestinal epithelial barrier leads to inflammatory diseases, which include inflammatory bowel disease (IBD) and necrotizing enterocolitis (NEC) [1,2]. Intestinal host defense mechanisms are subdivided into extracellular (mucus) and cellular (mucosa) components [3]. Inside the gut lumen, the mucus layer that covers the epithelium is mainly composed of mucins, a family of heavily glycosylated proteins. In the colon and the stomach, the mucus is comprised of two layers, inner and outer, as opposed to a single-layer in the small intestine [4]. In the colon, the inner mucus layer is dense, attached to the epithelium, and contains secretory immunoglobulin A and antimicrobial proteins that prevent the invasion of bacteria [5]. The outer mucus layer is loose, non-attached and is the habitat for microbiota [4]. The cellular intestinal barrier is composed of a monolayer of epithelial cells lining the gastrointestinal tract and is the primary physical barrier between microbiota and the underlying lamina propria [6]. Gut permeability is crucial for nutrient and water absorption in the intestine but epithelial integrity is essential for prevention of the entrance of luminal contents such as bacteria and their products through the large intestine. The apical junctional complex (AJC) regulates the intestinal permeability and is comprised of both tight junctions and adherens junctions which form the AJC [3].

The tight junction is the most apical junctional complex of the intestinal epithelium barrier and plays a critical role in the regulation of permeability and prevention of pathogen invasion. Transmembrane proteins, claudins, occludin, and junctional adhesion molecule (JAM) as well as the cytoplasmic scaffolding proteins zonular occludens (ZO-1, ZO-2, and ZO-3) form the tight junction complex [7]. In fact, it has been reported that tight junction proteins are dysregulated in diseases such as IBD and celiac disease, which are commonly associated with a leaky gut [1]. Specifically, decreased levels of ZO-1 were observed in the luminal surface epithelium of colons from IBD patients as compared to non-IBD controls [8,9].

Control of permeability of the epithelial barrier by functional tight junction complexes is especially critical to inhibit or prevent infection by specific bacterial strains. For example, *Citrobacter rodentium* is an attaching and effacing bacterial pathogen in mice that resembles human enteropathogenic *E.coli* (EPEC). EPEC is known to cross the epithelium through the epithelial tight junctions [10]. Therefore, the tight junction complex plays a critical role in preventing EPEC infection in humans and *Citrobacter* infection in mice. In fact, many bacteria, including EPEC, *Salmonella*, and *Helicobacter pylori* are known to have virulent mechanisms that alter tight junctions of host epithelium by decreasing or dissociating ZO-1 proteins [11].

ZO proteins are plaque proteins, which act as adaptors that connect transmembrane tight junction proteins to the actin cytoskeleton. ZO-1 plays a central role in clustering and stabilizing the tight junction complex by binding to claudins and occludin, as well as by forming dimers with other ZO proteins [12,13]. Studies have shown that decreased levels of ZO-1 correlate with increased permeability *in vitro* [14,15]. Furthermore, it has been found that the changes in phosphorylation of ZO-1 modify the assembly of complexes, resulting in

alterations in the permeability of cell monolayers. [16–19]. However, the reported levels of ZO-1 phosphorylation and tight junction complex association are not always consistent. This suggests that both cell type as well as the level of phosphorylation due to multiple phosphorylation sites within the ZO-1 protein are important [19]. In epithelial cells, ZO-1 phosphoryaltion mediates the dissociation of ZO-1 from the occludin complex, resulting in an increased permeability [18,20].

Hyaluronan (HA) is a glycosaminoglycan polymer, which consists of repeating disaccharides of β-glucuronic acid and N-acetylglucosamine. HA of varying sizes is synthesized by HA synthases (HAS1,2 and 3) and is commonly present as a high molecular weight polymer of up to 10,000 kDa in the extracellular matrix of most tissues [21–23]. During inflammation, large sized HA polymers are degraded into small fragments by specific enzymes, as well as through non-specific pathways, including reactive oxygen species (ROS)-mediated mechanisms [24,25]. The function of HA is known to be size-specific, and in general, small fragments of HA are pro-inflammatory, pro-angiogenic, and induce cell proliferation, while large polymers of HA have the opposite effects and promote homeostasis [21].

In addition to the extracellular matrix, HA fragments (<500 kDa) are also present in human milk [26,27], which indicates that the developing human intestine is meant to be exposed to naturally occurring HA. This suggests that HA may be beneficial for newborns, similar to other human milk oligosaccharides that are known to protect infants from infections [28]. A focus of our research is to investigate the mechanisms through which HA, both milk-derived and pure biosynthetic, mediate gut protection.

In agreement with the concept of HA mediated gut protection, Reich et al. have shown that intermediate molecular weight HA (750 kDa), when delivered *via* intraperitoneal injection, promotes colonic epithelium growth and protection from colitis in mice [29,30]. We have previously reported that hyaluronan purified from human milk (milk HA) enhances innate intestinal epithelial antimicrobial defense *in vitro* and *in vivo* and inhibits *Salmonella* infection *in vitro* [26]. In addition, we have established that a specific sized commercially available highly purified biosynthetic HA (HA 35 kDa) can mimic the protective effects of HA from human milk *in vitro* and *in vivo*. Both the biosynthetic HA 35 kDa (HA35) as well as natural milk HA promote the expression of an innate antimicrobial peptide human β-defensin 2 (hBD-2) in intestinal epithelial cells (HT29) in a time- and dose-dependent manner [26,31]. Furthermore, oral administration of HA35, as well as milk HA, promotes the expression of an hBD-2 ortholog in the colonic epithelium of wild-type mice [26,31].

We now hypothesize that, in addition to the induction of hBD-2, HA35 treatment leads to upregulation of additional defense mechanisms. In this study, we demonstrate that administration of HA35 in mice induces the expression of ZO-1 in a size specific manner within the colonic epithelium. This ZO-1 inducing effect of HA35 may be a novel mechanism through which how HA35 treatment protects mice from *Citrobacter rodentium* infection. Importantly, HA35-mediated ZO-1 induction occurs *in vivo* even during the challenge of *Citrobacter* infection and DSS-induced colitis. Moreover, increased intestinal permeability following DSS treatment is significantly abrogated in HA35-treated mice

compared to water fed controls, giving further evidence for functional effects of HA35 dietary supplementation on enhancing intestinal epithelial barrier integrity.

2. Results

2.1. HA35 treatment protects mice from Citrobacter rodentium infection

Our group previously showed that HA treatment enhanced antibacterial activity in gut epithelial cells. We have found that HA35 treatment increases hBD-2 expression in human colonic epithelial cells and mBD-3 *in vivo* [31]. Furthermore, milk HA treatment inhibits *Salmonella* infection *in vitro* in a colonic epithelial cell line [26]. Therefore we wanted to determine whether HA35 treatment affects intestinal bacterial infection *in vivo*, and therefore used the *Citrobacter rodentium* infection model established by the Vallance group [32]. We measured loss of body weight (%) as an indicator of the severity of infection and also measured recoverable *Citrobacter* in stool. Mice were gavaged with water or HA35 once daily, for 5 days pre-infection and during the post-infection period. Animal weights were recorded daily post-infection. The results show that the water-treated control mice lost weight immediately post-infection (Fig. 1A). However, HA35-treated mice lost significantly less weight compared to water-treated mice (Fig. 1A). Additionally, comparison of colonies grown from feces collected from the infected mice shows that the HA35-treated group had a ~50% decrease in live *Citrobacter* at days 4 and 6 post infection (Fig. 1B). Furthermore, we asked whether the levels of *Citrobacter* present in the colon changed with HA35 treatment and whether they correlated with bacterial analysis of stool samples. We identified *Citrobacter* in colon sections by immunostaining with anti-*Citrobacter* antiserum, an antibody that recognizes O152 antigen on *Citrobacter*. Non-infected mouse colon was used as a non-specific staining control. The immunodetection results show that the water-treated control mice have overall higher number *Citrobacter* residing on the surface epithelium compared to HA35-treated mice (Fig. 1C). Importantly the staining in water-treated mice seemed to be located further into the crypts implying greater bacterial invasion. When sections were viewed under higher magnification, *Citrobacter* was observed in the subepithelial area in colons of mice treated with water whereas *Citrobacter* was mostly restricted to the surface epithelium of colons of HA35-treated mice (Fig. 1C). These results show that HA35 treatment reduces *Citrobacter rodentium* infection in mice and suggest that it prevents *Citrobacter* from invading into crypts and subepithelial regions.

2.2. Hyaluronan (HA) induces ZO-1 expression in mouse intestinal epithelium of distal colon in vivo in a size dependent manner

Attaching/effacing (AE) bacteria, such as *Citrobacter rodentium*, are non-cell invading bacteria that alter the permeability of intestinal epithelium and evidence suggests that AE bacteria can cross through colonic epithelial junctions [10]. Our data indicate that HA35 treatment prevents *Citrobacter* from being able to invade into the subepithelial area (Fig. 1C), suggesting that HA treatment modulates the tightness of epithelial barrier. To determine whether HA treatment affects the levels of tight junction proteins in colonic epithelium, we used both fluorescence histochemistry and immunoblot analysis. The expression levels of tight junction proteins in proximal, transverse, and distal colons of healthy C57/Bl6 mice gavaged with 300μg of various sizes of HA (4.7, 16, 35, 74, and 2000 kDa) once daily for 3

days were examined. By performing immunofluorescent staining for the tight junction proteins, claudins 1, 2, and 3, occludin and ZO-1 in colon sections, we found no change in protein expression or cell location of claudins 1, 2, and 3 or occludin (data not shown). However, HA35 significantly and specifically induced ZO-1 expression, in the distal colon (Fig. 2A and 2B); increased ZO-1 was not observed in proximal or transverse colons (data not shown). Strikingly, treatment with large size HA, that is HA2000, did not affect ZO-1 expression in colonic epithelium (Fig. 2A and 2B). Quantification of immunofluorescent staining revealed that the treatment of mice with several small sizes of HA (4.7, 16, 35, 74 kDa) increased ZO-1 expression in the distal colon in some of the treated animals, but HA35 treatment showed the most consistently potent induction of ZO-1, and reached statistically significant levels (Fig. 2B). To further confirm the histological findings, we performed Western blot analysis for ZO-1 in lysates of distal colon tissue from mice treated with water or HA35 for five consecutive days (300μg/day). Villin-1, which is an epithelial cell marker, was used to normalize ZO-1 expression levels to colonic epithelial cells from whole colon lysates. The epithelial expression of ZO-1 protein was significantly increased in HA35-treated mice as compared to control animals treated with water (Fig. 2C). Together, these data indicate that HA35 treatment increases ZO-1 expression levels in colonic epithelium of the distal colon in healthy mice.

2.3. HA35 treatment enhances ZO-1 expression in disease models of mice

Next, since HA35 treatment protected mice from *Citrobacter* infection (Fig.1), we tested whether ZO-1 expression is increased *in vivo* in *Citrobacter* infected mice treated with HA35. We found that there was a pronounced increase in expression levels of ZO-1 protein in distal colon of *Citrobacter* infected mice (Fig. 3).

Additionally, we wanted to test whether HA35 also promotes ZO-1 expression in an additional inflammation model, the DSS-induced colitis model. DSS is a chemical agent that damages epithelium and facilitates bacterial activation of intestinal inflammation. We orally administrated mice with water or HA35 (300μg/mouse) once per day for 5 days and then administrated 2.5% DSS in the drinking water for 3 days while gavaging water or HA35 once daily during DSS administration [33]. We collected proximal, transverse, and distal colons from mice and immunostained for ZO-1. Analysis of ZO-1 expression levels revealed that HA35 treatment significantly increases ZO-1 expression in mice at the early stage of DSS-induced colitis when the colonic epithelium is not yet destroyed (Fig. 4). Strikingly, HA35 treatment promoted the expression of ZO-1 not only in the distal colon but also in the transverse colon of the DSS-induced mice (Fig. 4). As noted in figure 2, we did not observe HA-mediated induction of ZO-1 in the transverse colon of healthy mice and only the distal colon showed protein induction with HA treatment. This might be due to a higher constitutive expression of ZO-1 in the transverse colon than in the distal colon of healthy mice that made detection of differences harder to measure. A previous report demonstrated that 3% DSS treatment reduces ZO-1 expression in mouse colons starting on day 1 and results in total absence on day 7 [34]. We also observed decreased ZO-1 expression in transverse colon with the DSS treatment and therefore we were able to detect ZO-1 induction with HA35 treatment. Collectively, our data (Fig. 3 and 4) indicate that treatment

with HA35 promotes significant increases in ZO-1 expression in colonic epithelium of mice challenged with *Citrobacter* and with DSS, in addition to unchallenged healthy mice.

2.4. HA35 treatment does not change the intestinal permeability in healthy mice but reduces it in DSS-treated mice

Studies have shown that disrupted or decreased expression of ZO-1 resulted in increased paracellular permeability *in vitro* [12,35]. Furthermore, a report demonstrated that an increase in ZO-1 protein expression in colonic epithelium was sufficient to inhibit intestinal permeability *in vivo* [34]. Since we established that HA35 treatment enhances ZO-1 protein expression (Fig. 2), we next wanted to investigate the effect of HA35 treatment on intestinal barrier function by measuring leakiness. We employed the standard FITC-dextran gut permeability assay [32] that assesses translocation of 4 kDa FITC-dextran from the GI tract to serum during a 4 h window. We measured the concentration of FITC-dextran in the serum of healthy mice that had been treated with 300μg of HA35 or water once daily for 5 days. We found that FITC-dextran concentrations in serum did not significantly differ between water and HA35-treated healthy mice (Fig. 5A), suggesting that HA35 treatment does not alter the intestinal permeability of healthy mice with an already intact barrier.

To determine whether HA35 can protect under conditions known to disrupt barrier function, we again employed the DSS treatment model. Mice were gavaged with HA35 (300μg, once daily) or water for 5 days before initiation and during the 3 days of 2.5% DSS drinking water treatment. Again, FITC-dextran was administered 4 h before the end of the experiment and serum levels determined. As seen in Fig. 5B, in water-treated mice there was an overall statistically significant increase in serum FITC-dextran levels in serum with DSS treatment, although there was obvious variability among the mice. However the HA35-treated group had some of the lowest serum FITC-dextran levels and displayed much less variability. These results suggest that HA35 may promote barrier function under damaging conditions, consistent with the role of ZO-1.

3. Discussion

Our previous studies have demonstrated that HA treatment enhances protection of colonic epithelium, in part *via* promoting expression of the antimicrobial peptide human beta defensin-2 (hBD-2) and inhibiting *Salmonella enterica* intracellular infection [26,31]. In the present study, we investigated whether HA treatment has additional protective effects that involve modulation of barrier function by intestinal epithelium. In this report, we show that HA35 treatment protects mice from *Citrobacter rodentium*, an organism that infects paracellularly across the epithelium barrier. We also found that HA35 treatment specifically and significantly increases the expression of ZO-1, a regulator of tight junctions *in vivo*: 1) in healthy murine colonic epithelium; 2) during early stages of *Citrobacter* infection; and 3) during DSS-induced colitis. Additionally, our data revealed that HA35 treatment may reduce the DSS-induced increase in colonic permeability.

The specific effect of intermediate-sized HA (35 kDa) on ZO-1 induction observed *in vivo* confirms results from an *in vitro* study by Zahm *et al.* [36]. In their report the authors showed that treatment of cultured human lung epithelial cells with HA 40 kDa increases

expression of ZO-1. Importantly, and similar to our findings, the authors showed that another large form, HA1000 kDa, did not enhance the expression of ZO-1 [36]. Additionally, Ghazi *et al*. [37] also reported that medium molecular weight HA (100~200 kDa) treatment increases ZO-1 expression in cultured human skin keratinocytes, although that study did not include the ~35 kDa HA. To our knowledge, our report is the first to demonstrate that HA treatment mediates enhanced ZO-1 expression in colonic epithelium, and that HA35 functions *in vivo*.

An as yet unanswered question is why the induction of ZO-1, or for that matter of human β-defensin-2, by HA is so size specific. HA is linear polymer of unmodified repeating disaccharides of N-acetyl glucosamine and glucuronic acid. HA35 contains ~175 monosaccharides, whereas HA2000 contains ~10,000. Theoretically each HA receptor recognizes a 6–10 sugar span of the polymer, no matter the length. One possible explanation in our *in vivo* system is that large HA cannot penetrate through the mucus layer of the intestinal epithelium, and therefore would be excluded from contacting receptors on epithelial cells. Conceivably, HA of smaller sizes is much more likely to traverse the charged glycan-rich surface layer, but only HA of the intermediate size would efficiently engage, or multimerize receptors to transmit appropriate signals for ZO1 upregulation. In the cell culture models previously reported, the cell glycocalyx may act as the barrier to the large molecular weight anionic HA polymer [38].

Citrobacter is a genus of attaching and effacing (A/E) bacteria that is known to cross the epithelial barrier *via* the paracellular route [10]. Therefore tightening of the epithelial barrier is likely to play an important role in preventing *Citrobacter* translocation. The epithelial barrier is regulated by apical junctional complexes, and among these the tight junction complex is the most apically located. The importance of ZO-1 and tight junctions for mucosal integrity is supported by a study that demonstrated that probiotic *Escherichia coli* Nissle 1917 (EcN) could upregulate ZO-1 and also protect mice from DSS-colitis, including the associated increase in gut permeability [39]. Interestingly, EcN 1917 produces heparosan which has the identical monosaccharides as HA but different glycosidic linkages [40,41]. Oral administration of heparosan has been shown to improve the gut health, which raises the question of whether heparosan may also affect ZO-1 expression in the intestinal epithelium similar to HA35 [42,43]. Our data demonstrate that oral HA35 treatment delivered once per day can protect mice from *Citrobacter rodentium* infection. In exploring the role of HA35 in modulation of tight junctions, we found specific increases in ZO-1 protein localized to the distal colon of healthy mice. Interestingly, Guttman *et al*. [44] showed that *Citrobacter rodentium* infection causes dissociation of ZO-1 from tight junction complexes and disruption of barrier function *in vivo*. Importantly, we found that water-treated mice had a higher incidence of crypt and subepithelium invasion of *Citrobacter*, compared to HA35-treated animals. Our report suggests that HA35 treatment may help with epithelial barrier tightening, and supports the possibility that HA35 treatment protects mice from *Citrobacter* infection by modulating tight junctions. Likely, HA35 treatment protects mice from bacterial infection using multiple mechanisms including induction of beta defensins [31], and epithelial junction modulation, and even perhaps in additional unexplored ways, for example by inducing mucin secretion.

Balanced intestinal permeability is critical for maintaining healthy barrier function. Increased colonic permeability augments the chance of bacterial invasion yet decreased permeability can impair normal absorption of water or nutrients [3]. Here, we examined the effect of HA35 treatment on colonic permeability *in vivo* because tight junctions are known to regulate the paracellular permeability. Importantly, HA35 treatment did not alter the overall intestinal permeability in healthy mice, suggesting that the induction of ZO-1 in the distal colon post HA35 treatment would not result in significant decrease in gut permeability. In our study, we used the FITC-dextran permeability assay, which is well established for measurement of intestinal permeability. When we examined the sections of colons from FITC-dextran injected mice, most of the absorbed FITC-dextran was detected in proximal or transverse colon rather than distal colon (data not shown). Therefore, we think that one possible reason why HA35 treatment did not significantly reduce FITC-dextran levels in the serum of healthy mice is because ZO-1 induction only occurs in distal colon. However, during DSS treatment where transverse and distal colon ZO-1 is reduced, HA35 has the opportunity to restore or maintain the levels of this apical junction protein.

Taken together, our study demonstrates a novel innate host defense mechanism induced by a highly purified HA35. Our data show that HA35 treatment enhances intestinal health by modulating the epithelial barrier integrity. The effect of HA35 is analogous to the effects of the probiotic *E.coli* Nissle, previously demonstrated to be able to enhance the intestinal barrier function including *via* the induction of ZO-1 and hBD-2 [39,45]. Our data supports the concept that HA35 may be useful as a dietary supplement for promoting intestinal health for individuals at high risk for infections due to dysregulated colonic permeability. Specifically, for IBD patients or babies with NEC where decreased ZO-1 levels are thought to contribute to the high incidence of bacterial infections, HA35 may be a generally safe prophylactic strategy to increase host defense [8,46,47].

4. Methods

4.1. Animals

All experiments were conducted according to protocols approved by Lerner Research Institute's Institutional Animal Care and Use Committee (IACUC). Wild type C57/Bl6 male mice (6 to 8 weeks old) were used in the experiments and all were purchased from Jackson Laboratory (Bar Harbor, ME).

4.2. HA preparation

Commercially available highly purified HA fragments (Lifecore Biomedical, LLC) were dissolved at 1.2mg/ml in the drinking water provided in our animal housing facility and kept on a shaker at 4°C overnight before being aliquoted and frozen in −80°C until use.

4.3. Citrobacter rodentium infection

The kanamycin (Km)-resistant *Citrobacter rodentium* strain DBS100 strain CR:lux was a kind gift of Dr. Bruce A. Vallance (University of British Colombia) [48]. Two days before the infection, bacteria were streaked out on Luria-Bertani (LB) plates and the next day, a single colony was grown overnight in LB broth containing 50μg/ml of Km at 37°C on a

shaker. On the day of infection, 3×10^8 *Citrobacter* (150μl) per mouse was delivered by gavage. The CFU was confirmed by plating serial dilutions of the gavage stock on Km containing McConkey agar plates. Bacteria were grown overnight at 37°C and counted on the following day.

To determine the number of viable bacteria in the feces, fecal pellets were collected, weighed and homogenized in 500μl of PBS. Serially diluted (1:10~1:10^{-5}) samples were plated on Km containing McConkey agar plates. The number of colony forming units (CFU) was counted after overnight incubation at 37°C, and normalized to fecal weight.

4.4. DSS-induced epithelial damage

The dextran sulfate sodium (DSS) treatment was performed as previously described[33]. Briefly, mice received in-house water ad libitum in water bottles without or with 2.5% dextran sodium sulfate (#160110, MP Biomedicals, Solon, OH). Mice were weighed and monitored daily for signs of colitis. Mice were sacrificed according to IACUC approved methods on days 0 and 3. Colons were removed then fixed in ten times the tissue volume of molecular biology grade Histochoice (AMRESCO, Solon, OH) for overnight prior to paraffin embedding and tissue sectioning.

4.5. Immunofluorescence staining

Cut tissue sections (5μ) were deparaffinized by repeated dipping in the following solutions: Clear-Rite 3 (2 × 3mins), Flex 100 (2mins, 1min), Flex 95 (2mins, 1min) (Richard Allanermo Scientic, Kalamazoo, MI), and tap water. Sections were incubated in blocking solution of Hank's buffered saline solution containing 2% Fetal Bovine Serum (HBSS+ 2% FBS) for 30 minutes at room temperature. Primary antibodies were diluted in HBSS+ 2% FBS, applied to the sections and incubated at 4°C for overnight in a humidified chamber. For *Citrobacter* detection, rabbit anti-*Citrobacter* antiserum (Statens Serum Institute, Copenhagen, Denmark), that recognizes O-antigen (O152) expressed on *Citrobacter*, was used at a 1:200 dilution [49,50]. For ZO-1 detection, affinity purified rabbit polyclonal antibody against ZO-1 (ThermoFisher Scientific, Waltham, MA) was used at a 1:50 dilution. After primary antibody exposure, sections were washed with HBSS three times for 5 minutes each and then incubated with secondary antibody, goat anti-rabbit Alexa 568 (ThermoFisher Scientific, Waltham, MA) (1:1000 dilution in HBSS+ 2% FBS), for 1hr at room temperature. Slides were again washed in HBSS three times for 5 mins each. After washing, nucleus staining and mounting were done using Vectashield with DAPI (Vector laboratories, Burlingame, CA). Images of ZO-1 stained sections were obtained using a Leica DM5500B upright microscope equipped with a Leica DFC425C camera and LAS software (Leica Microsystems, GmbH, Wetzlar, Germany) and a Retiga SRV Cooled CCD camera and QCapture Plus software (QImaging, Surrey, BC Canada). Images of *Citrobacter* (low magnification) were acquired using a Leica TCS-SP8-AOBS inverted confocal microscope (Leica Microsystems, GmbH, Wetzlar, Germany). Images of *Citrobacter* (high magnification) were obtained using a Leica TCS-SP5II upright confocal/multiphoton microscope (Leica Microsystems, GmbH, Wetzlar, Germany). The quantification of image fluorescence was conducted using Image-Pro Plus computer software (Media Cybernetics, Rockville, MD).

4.6. Immunoblotting detection of ZO-1

Mouse colon lysates were made from 1cm-length of mouse distal colons that were homogenized in 2× RIPA buffer (Cell Signaling Technology, Danvers, MA) containing 1× Halt Phosphatase inhibitor cocktail (ThermoFisher Scientific, Waltham, MA) and 1× Protease inhibitor cocktail (P8340, Sigma-Aldrich, St. Louis, MO). A Pellet Pestle cordless motor (Fisherbrand, Pittsburgh, PA) was used to homogenize the tissue on ice and the remaining undissolved tissue was removed with forceps. Samples were centrifuged for 10 mins at 14000 rpm and then the supernatants were collected. 13μl of each sample was mixed with 5μl of lithium dodecyl sulfate (LDS) sample buffer (4×) (ThermoFisher Scientific) and 2μl of Sample reducing agent (10×) (ThermoFisher Scientific). Mixed samples were boiled at 95°C for 10 mins. Proteins were separated on SDS-PAGE using 4~15% Mini-PROTEAN® TGX™ Precast Gels (Biorad, Hercules, CA) run at a constant voltage of 100 V for 90 mins. Separated proteins were transferred at 4°C to 0.45mm PVDF membrane (Millipore, Billerica, MA) using the Trans-blot Turbo system (Biorad, Hercules, CA) using the preprogrammed protocol for high molecular weight proteins. PVDF membranes were blocked in PBST (PBS with containing 0.1% tween) containing 5% milk for one hour and then incubated with a rabbit polyclonal antibody against ZO-1 (Thermo Fisher Scientific, Waltham, MA) at 1:1000 or rabbit polyclonal antibody against Villin-1 (Cell signaling, Danvers, MA) at 4°C overnight on a shaker. Afterwards, membranes were washed with PBST 3 times, for 10 mins each, and then incubated with HRP-conjugated donkey polyclonal anti-rabbit IgG (GE Healthcare, Little Chalfont, UK) at 1:20,000 dilution in PBST containing 5% milk for 1hr at room temperature. Membranes were then washed with PBST 3 times for 10 mins each, and protein bands were visualized using Amersham ECL Prime Western Blotting Detection Reagent (GE Healthcare, Little Chalfont, UK).

4.7. FITC-dextran permeability assay

4 kDa FITC-dextran (Sigma-Aldrich, St. Louis, MO) was prepared by dissolving in sterile PBS at a concentration of 80 mg/ml. Mice were gavaged with 150μl 4 hrs prior to sacrificing and food was removed after gavage. Mice were then euthanized and blood was collected *via* aortic clip (thoracic cavity). BD Microtainer serum separators were used to collect serum. Collection tubes were spun down at room temp for 10 mins at 4100 rpm and serum from the top layer was collected and transferred into sterile tubes. The FITC-dextran standard curve was prepared by diluting the 80mg/ml stock gavage solution to the following concentrations in PBS: 800, 400, 200, 100, 50, 25, 12.5, 6.25, 3.12, 1.56, 0.78 and 0μg/ml. Standards and samples were loaded into Black 96well Micro Assay plate (Greiner Bio-one, Kremsmünster, Austria) and the florescence was quantified using FlexStation 3 (Molecular Devices, Sunnyvale, CA) fluorometer using excitation wavelength of 485nm and emission wavelength of 535nm.

4.8. Statistical Analysis

The statistical difference between groups was evaluated where appropriate by the unpaired one-tailed Student's *t* test or Mann-Whitney test to compare two groups and ANOVA for more than two groups as indicated. All error bars drawn indicate the standard error of mean

(SEM). All graphs and statistical analysis were done using GraphPad Prism version 5.0a (GraphPad Software, Inc, La Jolla, CA).

Acknowledgments

We thank Dr. Bruce A. Vallance for providing us with *Citrobacter rodentium* and Dr. Judy Drazba for microscopy assistance. We also thank the Cleveland Clinic Lerner Research Institute Imaging Core, which provided histology services.

Funding: This research was supported by the National Institutes of Health (HD061918, and the Programs of Excellence in Glycosciences Grant HL107147) as well as the Cleveland Clinic Innovators Research Fund (all to C de la M). This work utilized the *LeicaSP8 confocal microscope* that was purchased with funding from National Institutes of Health SIG grant [1S10OD019972-01]. This work utilized the *Leica SP5 confocal/multi-photon microscope* that was purchased with partial funding from National Institutes of Health SIG grant [1S10RR026820-01].

Abbreviations

HA35	Hyaluronan 35 kDa
EPEC	Enteropathogenic *E. coli*
ZO	Zonula occludens
JAM	Junctional adhesion molecule
DSS	Dextran sulfate sodium
IBD	Inflammatory bowel disease
NEC	Necrotizing enterocolitis
AJC	Apical junctional complex
hBD-2	Human β-defensin 2
Milk HA	Hyaluronan purified from human milk
ROS	Reactive oxygen species
A/E	Attaching/effacing

References

1. Groschwitz KR, Hogan SP. Intestinal barrier function: Molecular regulation and disease pathogenesis. Journal of Allergy and Clinical Immunology. 2009; 124:3–20. [PubMed: 19560575]
2. Petrosyan M, Guner YS, Williams M, Grishin A, Ford HR. Current concepts regarding the pathogenesis of necrotizing enterocolitis. Pediatr. Surg. Int. 2009; 25:309–318. [PubMed: 19301015]
3. Turner JR. Intestinal mucosal barrier function in health and disease. Nat Rev Immunol. 2009; 9:799–809. [PubMed: 19855405]
4. Johansson M, Sjövall H, Hansson GC. The gastrointestinal mucus system in health and disease. Nat Rev Gastroenterol Hepatol. 2013; 10:352–361. [PubMed: 23478383]
5. Johansson MEV, Larsson JMH, Hansson GC. The two mucus layers of colon are organized by the MUC2 mucin, whereas the outer layer is a legislator of host-microbial interactions. Proc. Natl. Acad. Sci. U.S.a. 2011; 108:4659–4665. [PubMed: 20615996]

6. Round JL, Mazmanian SK. The gut microbiota shapes intestinal immune responses during health and disease. Nat Rev Immunol. 2009; 9:313–323. [PubMed: 19343057]
7. Neunlist M, Van Landeghem L, Mahé MM, Derkinderen P, des Varannes SB, Rolli-Derkinderen M. The digestive neuronal-glial-epithelial unit: a new actor in gut health and disease. Nature Reviews Gastroenterology and Hepatology. 2013; 10:90–100. [PubMed: 23165236]
8. Gassler N, Rohr C, Schneider A, Kartenbeck J, Bach A, Obermüller N, et al. Inflammatory bowel disease is associated with changes of enterocytic junctions. AJP: Gastrointestinal and Liver Physiology. 2001; 281:G216–G228.
9. Kucharzik T, Walsh SV, Chen J, Parkos CA, Nusrat A. Neutrophil Transmigration in Inflammatory Bowel Disease Is Associated with Differential Expression of Epithelial Intercellular Junction Proteins. The American Journal of Pathology. 2001; 159:2001–2009. [PubMed: 11733350]
10. Li Q, Zhang Q, Wang C, Li N, Li J. Invasion of enteropathogenic Escherichia coli into host cells through epithelial tight junctions. FEBS Journal. 2008; 275:6022–6032. [PubMed: 19016848]
11. Guttman JA, Finlay BB. Tight junctions as targets of infectious agents. Biochimica Et Biophysica Acta (BBA) - Biomembranes. 2009; 1788:832–841. [PubMed: 19059200]
12. Rodgers LS, Beam MT, Anderson JM, Fanning AS. Epithelial barrier assembly requires coordinated activity of multiple domains of the tight junction protein ZO-1. J. Cell. Sci. 2013; 126:1565–1575. [PubMed: 23418357]
13. Ulluwishewa D, Anderson RC, McNabb WC, Moughan PJ, Wells JM, Roy NC. Regulation of tight junction permeability by intestinal bacteria and dietary components. J. Nutr. 2011; 141:769–776. [PubMed: 21430248]
14. Youakim A, Ahdieh M. Interferon-gamma decreases barrier function in T84 cells by reducing ZO-1 levels and disrupting apical actin. Am. J. Physiol. 1999; 276:G1279–G1288. [PubMed: 10330020]
15. Neunlist M, Toumi F, Oreschkova T, Denis M, Leborgne J, Laboisse CL, et al. Human ENS regulates the intestinal epithelial barrier permeability and a tight junction-associated protein ZO-1 via VIPergic pathways. AJP: Gastrointestinal and Liver Physiology. 2003; 285:G1028–G1036.
16. Stevenson BR, Anderson JM, Braun ID, Mooseker MS. Phosphorylation of the tight-junction protein ZO-1 in two strains of Madin-Darby canine kidney cells which differ in transepithelial resistance. Biochem. J. 1989; 263:597–599. [PubMed: 2597123]
17. Van Itallie CM, Balda MS, Anderson JM. Epidermal growth factor induces tyrosine phosphorylation and reorganization of the tight junction protein ZO-1 in A431 cells. J. Cell. Sci. 1995; 108(Pt 4):1735–1742. [PubMed: 7542259]
18. Rao RK, Basuroy S, Rao VU, Karnaky KJ Jr, Gupta A. Tyrosine phosphorylation and dissociation of occludin-ZO-1 and E-cadherin-beta-catenin complexes from the cytoskeleton by oxidative stress. Biochem. J. 2002; 368:471–481. [PubMed: 12169098]
19. Rincon-Choles H, Vasylyeva TL, Pergola PE, Bhandari B, Bhandari K, Zhang J-H, et al. ZO-1 expression and phosphorylation in diabetic nephropathy. Diabetes. 2006; 55:894–900. [PubMed: 16567508]
20. Sallee JL, Burridge K. Density-enhanced phosphatase 1 regulates phosphorylation of tight junction proteins and enhances barrier function of epithelial cells. J. Biol. Chem. 2009; 284:14997–15006. [PubMed: 19332538]
21. Stern R, Asari AA, Sugahara KN. Hyaluronan fragments: an information-rich system. Eur. J. Cell Biol. 2006; 85:699–715. [PubMed: 16822580]
22. Vigetti D, Viola M, Karousou E, De Luca G, Passi A. Metabolic control of hyaluronan synthases. Matrix Biol. 2014; 35:8–13. [PubMed: 24134926]
23. Iozzo RV, Schaefer L. Proteoglycan form and function: A comprehensive nomenclature of proteoglycans. Matrix Biol. 2015; 42:11–55. [PubMed: 25701227]
24. Cyphert JM, Trempus CS, Garantziotis S. Size Matters: Molecular Weight Specificity of Hyaluronan Effects in Cell Biology. Int J Cell Biol. 2015; 2015:563818–563818. [PubMed: 26448754]
25. Hascall VC, Wang A, Tammi M, Oikari S, Tammi R, Passi A, et al. The dynamic metabolism of hyaluronan regulates the cytosolic concentration of UDP-GlcNAc. Matrix Biol. 2014; 35:14–17. [PubMed: 24486448]

26. Hill DR, Rho HK, Kessler SP, Amin R, Homer CR, McDonald C, Cowman MK, de la Motte CA. Human milk hyaluronan enhances innate defense of the intestinal epithelium. Journal of Biological Chemistry. 2013; 288:29090–29104. [PubMed: 23950179]
27. Yuan H, Amin R, Ye X, de la Motte CA, Cowman MK. Determination of hyaluronan molecular mass distribution in human breast milk. Anal. Biochem. 2015; 474:78–88. [PubMed: 25579786]
28. Bode L. Human milk oligosaccharides: every baby needs a sugar mama. Glycobiology. 2012; 22:1147–1162. [PubMed: 22513036]
29. Zheng L, Riehl TE, Stenson WF. Regulation of Colonic Epithelial Repair in Mice by Toll-Like Receptors and Hyaluronic Acid. Ygast. 2009; 137:2041–2051.
30. Riehl TE, Ee X, Stenson WF. Hyaluronic acid regulates normal intestinal and colonic growth in mice. AJP: Gastrointestinal and Liver Physiology. 2012; 303:G377–G388.
31. Hill DR, Kessler SP, Rho HK, Cowman MK, de la Motte CA. Specific-sized Hyaluronan Fragments Promote Expression of Human -Defensin 2 in Intestinal Epithelium. Journal of Biological Chemistry. 2012; 287:30610–30624. [PubMed: 22761444]
32. Bhinder G, Sham HP, Chan JM, Morampudi V, Jacobson K, Vallance BA. The Citrobacter rodentium mouse model: studying pathogen and host contributions to infectious colitis. J Vis Exp. 2013:e50222. [PubMed: 23462619]
33. Kessler SP, Obery DR, De La Motte C. Hyaluronan Synthase 3 Null Mice Exhibit Decreased Intestinal Inflammation and Tissue Damage in the DSSInduced Colitis Model. Int J Cell Biol. 2015; 2015:745237–745213. [PubMed: 26448758]
34. Poritz LS, Garver KI, Green C, Fitzpatrick L, Ruggiero F, Koltun WA. Loss of the Tight Junction Protein ZO-1 in Dextran Sulfate Sodium Induced Colitis. Journal of Surgical Research. 2007; 140:12–19. [PubMed: 17418867]
35. Van Itallie CM, Fanning AS, Bridges A, Anderson JM. ZO-1 stabilizes the tight junction solute barrier through coupling to the perijunctional cytoskeleton. Mol. Biol. Cell. 2009; 20:3930–3940. [PubMed: 19605556]
36. Zahm J-M, Milliot M, Bresin A, Coraux C, Birembaut P. The effect of hyaluronan on airway mucus transport and airway epithelial barrier integrity: potential application to the cytoprotection of airway tissue. Matrix Biol. 2011; 30:389–395. [PubMed: 21839834]
37. Ghazi K, Deng-Pichon U, Warnet J-M, Rat P. Hyaluronan fragments improve wound healing on in vitro cutaneous model through P2X7 purinoreceptor basal activation: role of molecular weight. PLoS ONE. 2012; 7:e48351. [PubMed: 23173033]
38. Shakya S, Wang Y, Mack JA, Maytin EV. Hyperglycemia-Induced Changes in Hyaluronan Contribute to Impaired Skin Wound Healing in Diabetes: Review and Perspective. Int J Cell Biol. 2015; 2015:701738–701711. [PubMed: 26448756]
39. Ukena SN, Singh A, Dringenberg U, Engelhardt R, Seidler U, Hansen W, et al. Probiotic Escherichia coli Nissle 1917 Inhibits Leaky Gut by Enhancing Mucosal Integrity. PLoS ONE. 2007; 2:e1308. [PubMed: 18074031]
40. Hickey AM, Bhaskar U, Linhardt RJ, Dordick JS. Effect of eliminase gene (elmA) deletion on heparosan production and shedding in Escherichia coli K5. Journal of Biotechnology. 2013; 165:175–177. [PubMed: 23583654]
41. Kane TA, White CL, DeAngelis PL. Functional characterization of PmHS1, a Pasteurella multocida heparosan synthase. J. Biol. Chem. 2006; 281:33192–33197. [PubMed: 16959770]
42. Duan R, Chen X, Wang F, Zhang T, Ling P. Oral administration of heparin or heparosan increases the Lactobacillus population in gut microbiota of rats. Carbohydr Polym. 2013; 94:100–105. [PubMed: 23544516]
43. Chen X, Ling P, Duan R, Zhang T. Effects of heparosan and heparin on the adhesion and biofilm formation of several bacteria in vitro. Carbohydr Polym. 2012; 88:1288–1292.
44. Guttman JA, Samji FN, Li Y, Vogl AW, Finlay BB. Evidence that tight junctions are disrupted due to intimate bacterial contact and not inflammation during attaching and effacing pathogen infection in vivo. Infection and Immunity. 2006; 74:6075–6084. [PubMed: 16954399]
45. Möndel M, Schroeder BO, Zimmermann K, Huber H, Nuding S, Beisner J, et al. Probiotic E. coli treatment mediates antimicrobial human beta-defensin synthesis and fecal excretion in humans. Mucosal Immunol. 2009; 2:166–172. [PubMed: 19129752]

46. Michielan A. Intestinal Permeability in Inflammatory Bowel Disease: Pathogenesis. Clinical Evaluation, and Therapy of Leaky Gut, Mediators of Inflammation. 2015; 2015:1–10. D. x2019, I. xe0.

47. Shiou S-R, Yu Y, Chen S, Ciancio MJ, Petrof EO, Sun J, et al. Erythropoietin protects intestinal epithelial barrier function and lowers the incidence of experimental neonatal necrotizing enterocolitis. Journal of Biological Chemistry. 2011; 286:12123–12132. [PubMed: 21262973]

48. Bergstrom KSB, Kissoon-Singh V, Gibson DL, Ma C, Montero M, Sham HP, et al. Muc2 protects against lethal infectious colitis by disassociating pathogenic and commensal bacteria from the colonic mucosa. PLoS Pathog. 2010; 6:e1000902. [PubMed: 20485566]

49. Luperchio SA, Newman JV, Dangler CA, Schrenzel MD, Brenner DJ, Steigerwalt AG, et al. Citrobacter rodentium, the causative agent of transmissible murine colonic hyperplasia, exhibits clonality: synonymy of C. rodentium and mouse-pathogenic Escherichia coli. J. Clin. Microbiol. 2000; 38:4343–4350. [PubMed: 11101562]

50. Hodgson A, Wier EM, Fu K, Sun X, Yu H, Zheng W, et al. Metalloprotease NleC Suppresses Host NF-κB/Inflammatory Responses by Cleaving p65 and Interfering with the p65/RPS3 Interaction. PLoS Pathog. 2015; 11:e1004705–23. [PubMed: 25756944]

Highlights

1. Oral administration of Hyaluronan 35 kDa (HA35) inhibits murine *Citrobacter rodentium* infection, a model of human enteropathogenic *E. coli*.
2. Biosynthetic HA fragments induce ZO-1 expression in the intestinal epithelium of the distal colon in healthy mice.
3. Oral HA35 treatment enhances epithelial ZO-1 expression in murine infection and colitis models.
4. Treatment with HA35 reduces the intestinal permeability in mouse intestine damaged with dextran sulfate sodium (DSS).
5. Treatment with HA35 promotes intestinal barrier function *in vivo*.

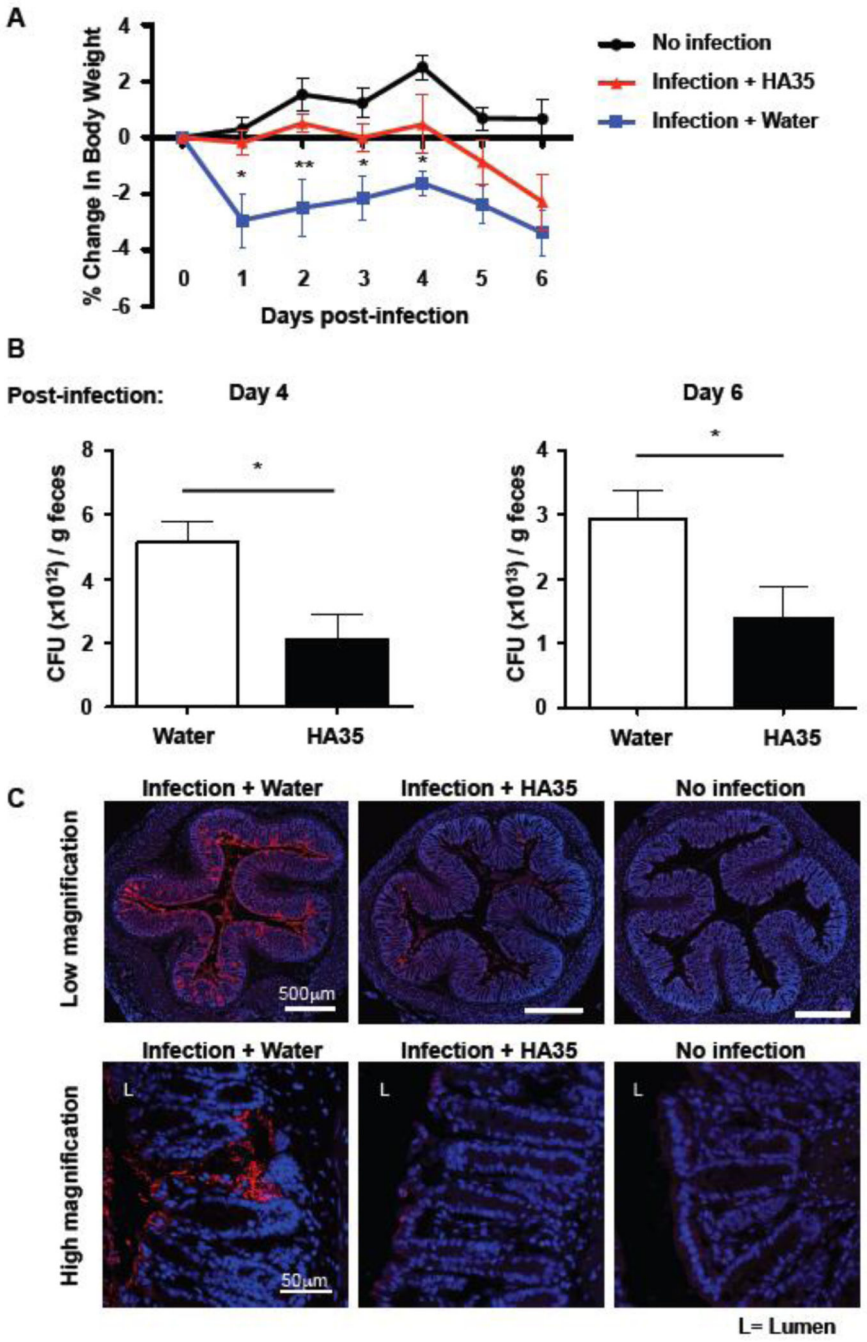

Figure 1. Oral administration of HA35 inhibits *Citrobacter rodentium* infection in adult mice

A. Mice were orally administered HA35 (300μg/mouse) or water once daily for 5 days by gavage before the infection and post infection. After pretreatment, *Citrobacter* (3×10^8 bacteria per mouse) were delivered by gavage. Mice were weighed daily post *Citrobacter* infection. Average body weight is calculated from 4 mice/group of non-infected mice and 6 mice/group of infected mice and data are combined from two independent experiments. Statistical analysis was done using a one-tailed unpaired t-test and the significance of differences is indicated in the figure (*, $p<0.05$, **, $p<0.01$). *Error bars=S.E.M.* **B**. The

number of kanamycin resistant *Citrobacter* in the stool of infected mice (n=3 per group) was determined by growth on kanamycin containing McConkey agar plates. Statistical analysis was done using the one-tailed unpaired t-test and the significance of differences is indicated in the figure (*, $p<0.05$). **C**. Colons were collected from mice treated with HA35 (300μg/mouse) or water once per day for 5 days before the infection and 7 days post infection. Distal colon sections from *Citrobacter* infected mice were immunostained for *Citrobacter* (red) and nuclei were stained blue (DAPI) as described in “Methods”, and non-infected mouse colons were used as negative bacterial staining controls. Low magnification images were generated with tile scanning fluorescent imaging and high magnification images were taken using confocal microscopy of a single plane.

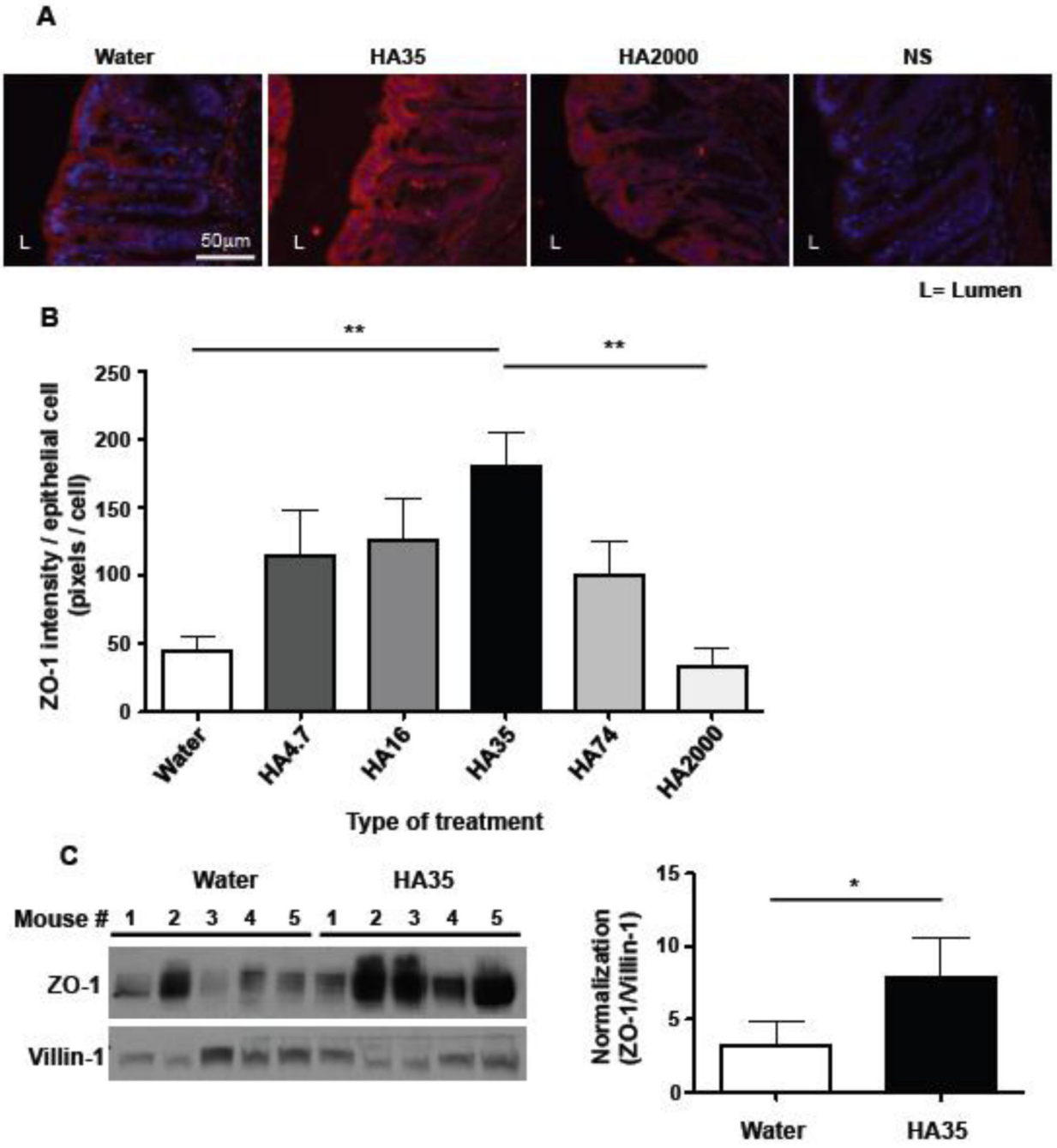

Figure 2. Oral delivery of low molecular weight HA to healthy mice increases ZO-1 expression in the distal colon in a size dependent manner

A. Sections of distal colon from wild type mice gavaged once daily with water or 300μg of multiple sizes of hyaluronan (HA) (4.7, 16, 35, 74, and 2000 kDa) for three days were immunostained for ZO-1 (red) and nuclei were stained blue (DAPI). Representative fluorescent micrographs show ZO-1 staining in the colonic epithelium of distal colons of mice treated with water or with HA35 or with HA2000. Non-specific (NS) indicates the secondary antibody staining control. **B**. Images were quantified using 3 stained sections per

mouse and 3 mice per group. ZO-1 staining intensity was measured as described in "Methods" and normalized to the number of epithelial cells by counting the number of epithelial cell nuclei. One-way ANOVA was used to test the significance of the differences between various sizes of HA-treated groups and water-treated group. (**, $p<0.01$). **C**. Western blot analysis of ZO-1 protein in distal colon tissue lysates from water- or HA35-treated wild type mice (300μg/mouse, once daily for 5 days). The same volume of each lysate was loaded per lane and the levels of ZO-1 were normalized to the expression levels of villin-1 (an epithelial cell marker). The densitometric quantification of ZO-1 and villin-1 protein bands was used to calculate the relative expression level of ZO-1 in epithelium of water and HA35-treated mice (5 mice per group). The one-tailed Mann-Whitney test was used to test the significance of difference between groups, and a significant difference is indicated in the figure (*, $p<0.05$). *Error bars=S.E.M.*

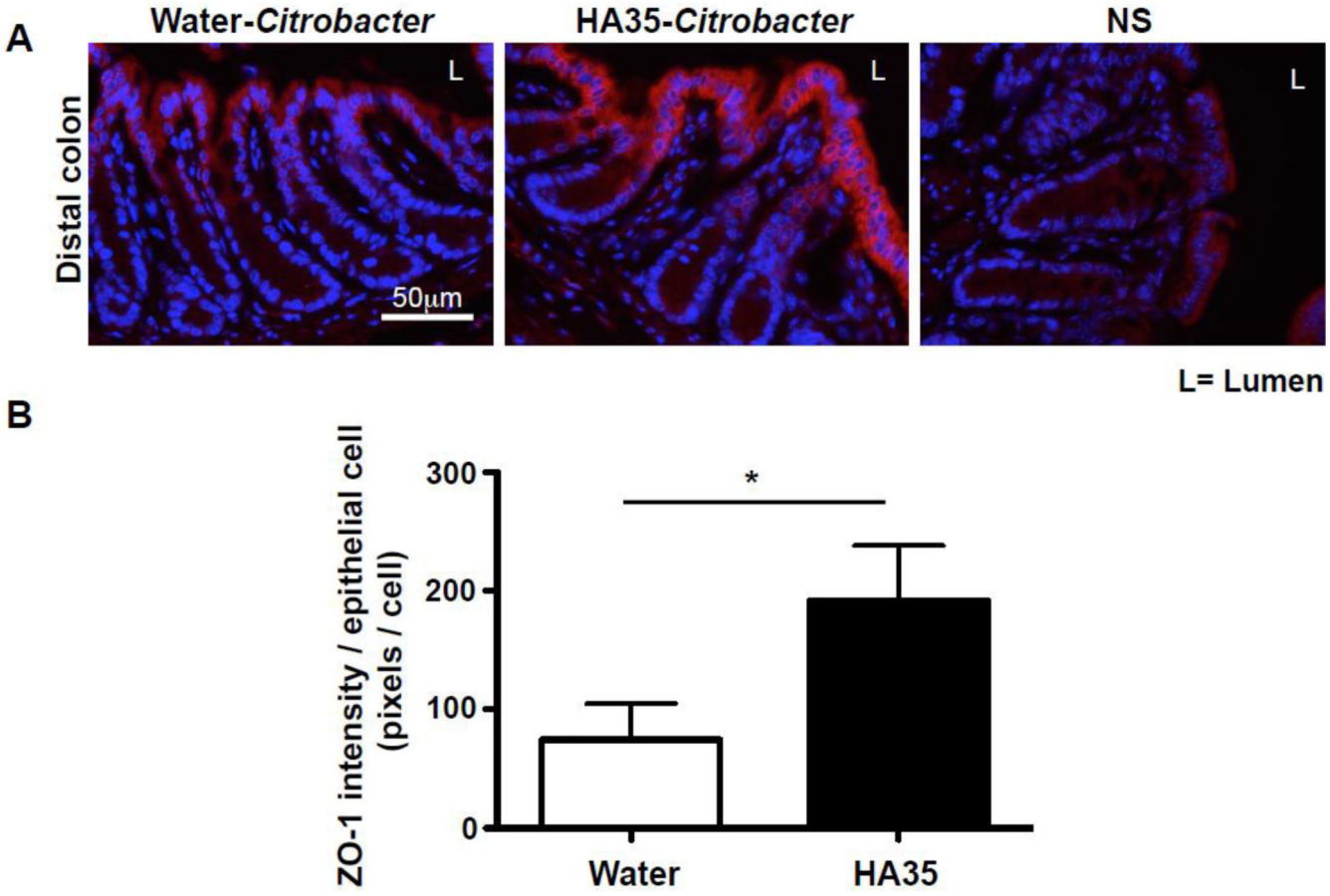

Figure 3. HA35 treatment increases ZO-1 expression in *Citrobacter rodentium* infected mice

A. Distal colon sections from *Citrobacter*-infected mice were immunostained for ZO-1(red) and nuclei were stained with DAPI (blue). Colons were collected from mice treated with HA35 (300μg/day) or water for 5 days before the infection and 4 days post infection. **B**. The quantification of ZO-1 intensity was performed on 2 stained sections per mouse, 6 mice per group and normalized to the number of epithelial cells. The statistical analysis was done using the one-tailed unpaired t-test. (*, $p<0.05$).

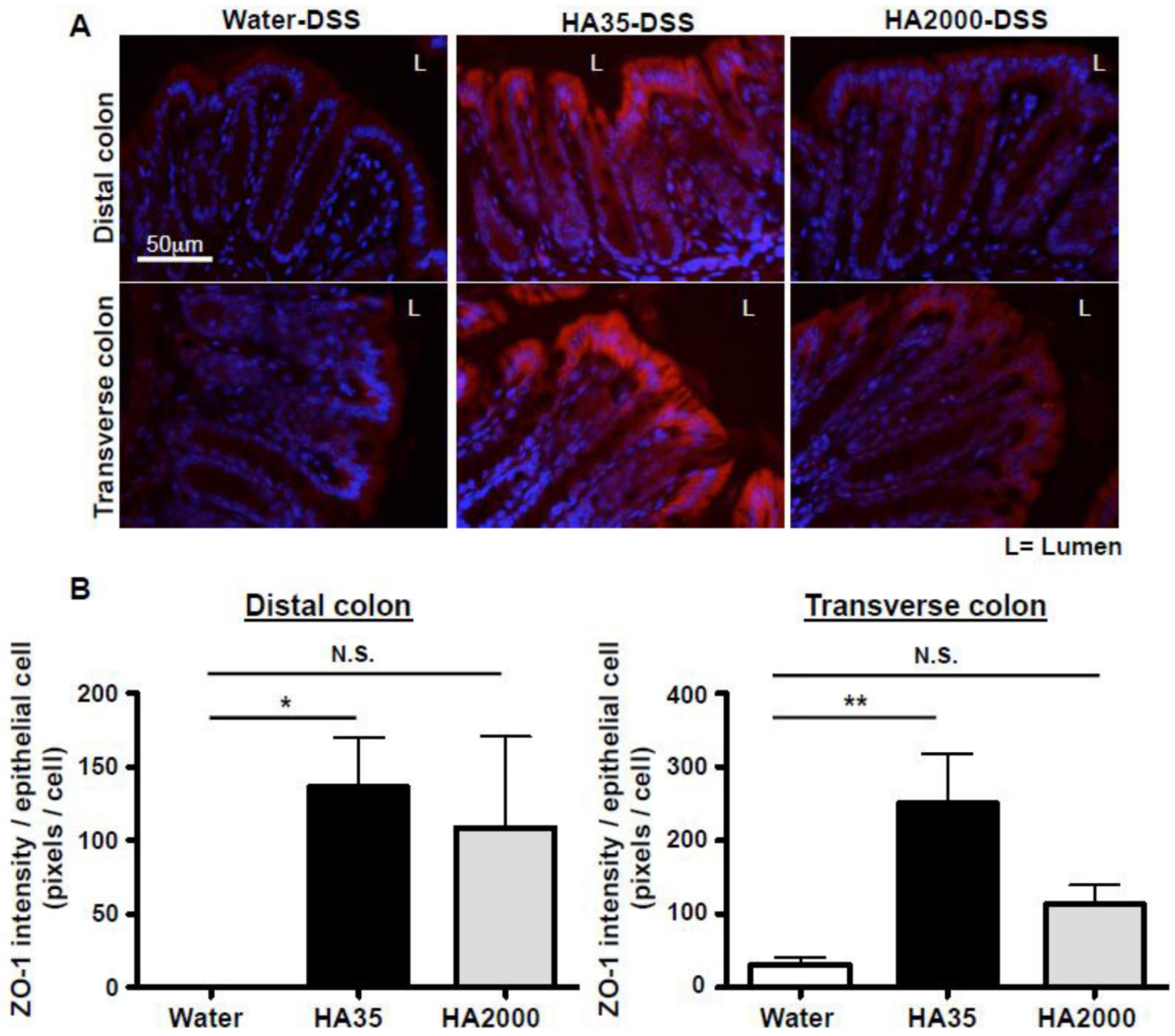

Figure 4. HA35 treatment increases ZO-1 expression in both the distal and transverse colon of DSS-treated mice

A. Groups of mice orally treated with HA35, HA2000 (300µg/mouse) or water once per day for 5 days before, as well as 3 days during 2.5% DSS administration were euthanized and their colons collected for histology. Transverse and distal colon sections were immunostained for ZO-1 (red) and nuclei were stained with DAPI (blue). **B**. The intensity of ZO-1 staining was quantified using 2 stained sections per mouse, 5 mice per group and normalized to the number of epithelial cells. One-way ANOVA was used to test the statistical significance of differences between HA-treated groups and the water-treated group. (*, $p<0.05$, **, $p<0.01$). *N.S.=not significant. Error bars=S.E.M.*

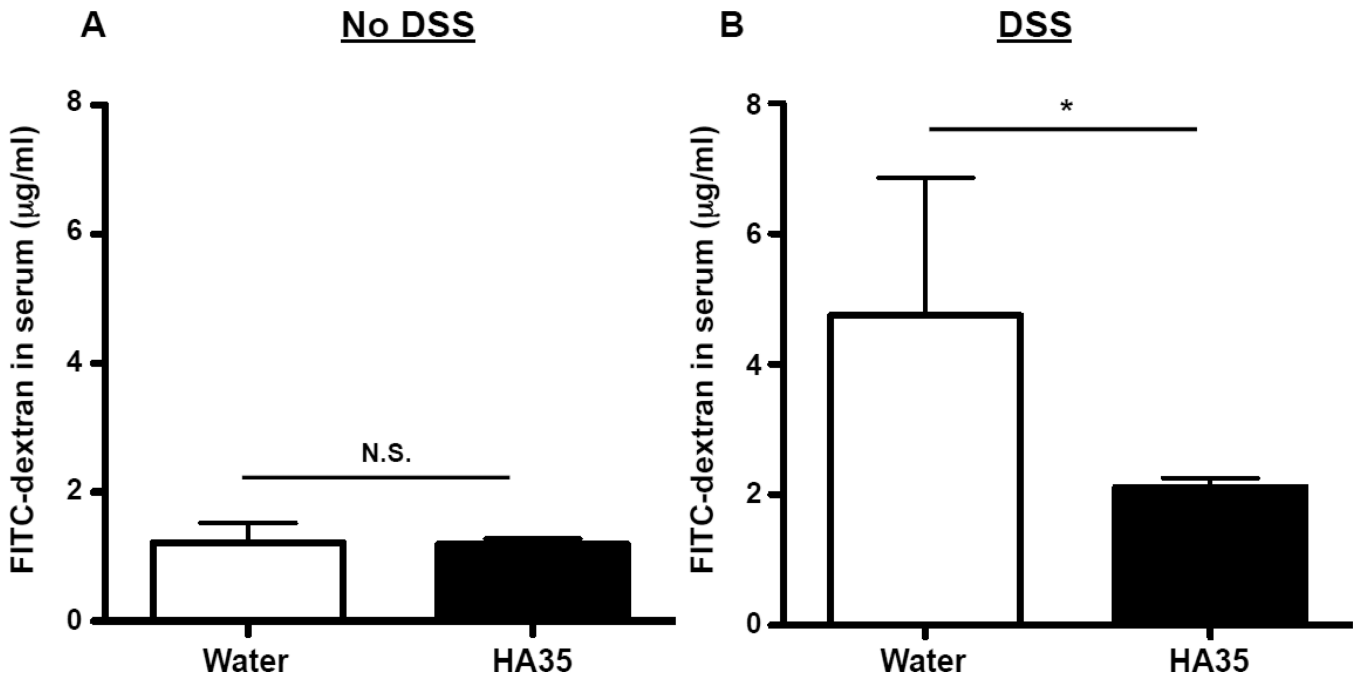

Figure 5. HA35 treatment prevents increased gut permeability during DSS exposure

A. Groups of mice (5 mice per group) were orally treated with HA35 (300μg/mouse) or water once per day for 5 days. On the day of euthanasia, mice were gavaged with FITC labeled-4kDa dextran 4 hours before serum collection. FITCdextran in serum was measured by spectroflurorometer. The serum of mice not given FITC-dextran (n=2) was used as the negative control, and the O.D. value was subtracted from all samples. Each dot represents an individual mouse in the graph. **B**. Groups of mice (5 mice per group) were orally treated with HA35 (300μg/mouse) or water once daily for 5 days before as well as 3 days during 2.5% DSS administration. On the day of euthanasia, mice were gavaged with FITC labeled-4 kDa dextran 4 hours before serum collection. The one-tailed Mann-Whitney test was used to test the significance of difference between groups, and a significant difference is indicated in the figure (*, $p<0.05$). *N.S.=not significant. Error bars=S.E.M.*